

Cellulose Nanofibers/SiO₂ nanocomposite: Preparation, Characterization and pH-Controlled Doxorubicin Delivery Properties

Roya Ferdose, Maryam Zirak*, Mahnaz Saraei

Department of Chemistry, Payame Noor University (PNU), Tehran, Iran

Article history:

Received: 25/June/2022

Received in revised form: 03/Dec/2022

Accepted: 06/Dec/2022

Abstract

Cellulose nanofibers/SiO₂ nanocomposite was prepared by extraction of cellulose nanofibers (CNFs) from *Yucca* leaves, followed by immobilization of SiO₂ nanoparticles on the surface of cellulose nanofibers denoted as SiO₂@CNFs. Prepared SiO₂@CNFs nanocomposite was characterized using various techniques, including Fourier Transform Infra-Red (FT-IR), X-Ray Diffraction (XRD), Thermogravimetric analysis (TGA), scanning electron microscopy (SEM), Transmission electron microscopy (TEM) and Energy Dispersive Spectroscopy (EDS) analysis, and used as controlled drug delivery system for the release of doxorubicin, an anticancer drug. CNFs exhibited higher loading level of doxorubicin (79.82%) than SiO₂@CNFs (72.67%), while CNFs exhibited rapid drug release, but SiO₂@CNFs showed controlled drug release properties. Doxorubicin release from CNFs is not pH sensitive, as CNFs released high content of doxorubicin, 94.0% and 88.0% within 5-7 h, at both pH values of 4.5 and 7.4, respectively. However, the release of doxorubicin from SiO₂@CNFs occurred slowly, and could be controlled by pH, as cumulative release percentage of doxorubicin from SiO₂@CNFs were measured to be 73.5% at pH = 4.5, while 17.07% at pH = 7.4 after 48 h. Doxorubicin release kinetic was studied by fitting the experimental data with well-known kinetic models, including zero order, first order, Higuchi, Korsmeyer-Peppas, Hixson-Corwell, Weibull and Gompertz models. Results revealed that the doxorubicin release from SiO₂@CNFs is well fitted with Higuchi and Hixson-Crowell models at pH = 4.5 and Hixson-Crowell model at pH = 7.4. Fitting the data using Korsmeyer-Peppas indicated the nonFickian diffusion of doxorubicin from SiO₂@CNFs at pH = 4.5 by n values of 0.4755, and Fickian type diffusion at pH = 7.4 by n values of 0.3359.

Keywords: Cellulose, SiO₂ nanoparticles, Drug delivery, Doxorubicin, Higuchi, Hixson-Corwell, Korsmeyer-Peppas.

*.Corresponding author: Assistant professor of organic chemistry, Department of Chemistry, Payame Noor University, Iran.
E-mail Address: m.zirak@pnu.ac.ir

1. Introduction

The easiest common drug delivery approach is oral administration, which includes more than 50% of drug delivery systems in the market. The ease of patient management is one of the most noticeable benefits of oral drug transformations. Applying a single dose for the entire treatment progress and carrying the drug directly to the target site are main features of an ideal drug system. Therefore, many attempts are made in order to create systems to be close to the ideal systems. Predictability and reliability in the drug delivery systems are two important aspects of controlled release, which provide well-ordered concentration of drug in the target tissue.[1] Advancement of the nanotechnology field led to the replacement of the conventional drug release systems, and has made significant improvements in the treatment of diseases. Generally, nanocarriers may protect drugs against degradation and increase drug efficiency by helping diffusion through the epithelium.[2] However, a preferred pattern of drug release can be achieved by modifying the surface and composition of nanocarriers,[3-5] in which degradable and biodegradable polymers play a significant role in the controlled release of drugs. Degradable polymers are divided into natural and synthetic types, that natural polymers have attracted much attention in view point of scientists.[6-10]

Due to the unique properties, including stability, non-toxicity, availability, renewability and biocompatibility and basic structure, cellulose as the most abundant polysaccharide, has found many applications in the field of drug delivery[11], dye removal [12, 13], and etc. In addition to the bulk cellulose, nano structured cellulose, such as cellulose nanocrystals (CNCs) and cellulose nanofibers (CNFs) are also well known, because of their exclusive properties. Due to the stability and non-toxicity, CNFs don't cause an immune response when implanted in the body tissues. Basically, the CNFs, prepared by separation of the fibers from the cellulose sources, include both amorphous and crystalline parts, which provide the flexibility and the high tensile strength of the CNFs, respectively. Because of the growing importance of controlled drug release, development of

novel sustainable drug delivery systems is of interest. In this context, due to the wide range of physicochemical properties, CNFs as a biocompatible polymeric material can be used to carry drugs to target tissues or even intracellular organs.[14-16] In this line, Valo et al. developed the integration of beclomethasone dipropionate nanoparticles coated with amphiphilic hydrophobin proteins into the CNFs aerogels, and investigated its drug delivery properties.[17] Recently, an electrospun poly(*N*-isopropylacrylamide)/ethyl cellulose nanofibers were developed as a thermoresponsive drug delivery system for release of ketoprofen.[18] In 2020, Allafchian and co-workers described poly vinyl alcohol-carboxymethyl cellulose nanofibers to controlled release of flufenamic acid.[19] In an interesting paper, Löbmann and Svagan reviewed the application of CNFs and its composited in the delivery of poorly soluble drugs.[20]

Among the many stable substances that have been studied for controlled drug delivery, silica-containing substances have received a lot of attention, because of their specific structure and surface properties, and also biodegradability. Silica is often the material of choice for the biological applications of mineral nanoparticles. As silica is able to store and gradually release drugs, silica based materials have attracted much attention for controlled drug release. In addition, silica based materials is used to increase the biocompatibility of drug delivery systems such as magnetic nanoparticles, biopolymers and micelles.[21, 22] In this context, Lin et al. reported *in vitro* release of aspirin using polymethylmethacrylate (PMMA)/silica composites.[23] Recently, a core-shell magnetic silica-coated hydroxyapatite composite, denoted as $\text{Fe}_3\text{O}_4@\text{SiO}_2@\text{HAp}$, was developed in order to pH-responsive drug delivery applications for captopril and ibuprofen drugs, as hydrophilic and hydrophobic drugs, respectively.[24] Due to the importance of the subject, there are many review articles on the application of silica based materials in controlled or stimuli-responsive drug delivery systems.[25-27]

Yucca plant is one of the most important sources of CNFs to controlled drugs release.[28, 29] In the present study, CNFs was extracted from *Yucca* and coated with silica

and its drug release properties for anti-cancer drug, doxorubicin, were investigated.

1. Experimental procedure

1.1. Materials and method

All chemicals were purchased from Merck and Sigma-Aldrich and used without any further purification. WinBomem, version 3.04 Galatic Industries Corporation, spectrometer was used for collecting the FT-IR spectra (KBr disc). X-ray diffraction (XRD) patterns were measured using a Bruker D8 Advance with CuK (α) radiation ($\lambda = 0.15406$ nm) in the range $4^\circ < 2\theta < 70^\circ$. VWGA3 TESCAN (20.0 KV) and Philips CM120 microscopes were used to prepare scanning electron microscope (SEM) images along with EDX analysis and transmission electron microscopy (TEM) images, respectively. Thermogravimetric (TGA) analyses were performed using a Linseis L81A1750 (Germany) at a heating rate of 10 °C/min under high purity nitrogen atmosphere from 50 to 800 °C. All absorption data was measurement by using two beams Shimadzu 1800 UV-Vis spectrophotometer using a 1 cm cell.

1.2. Preparation of SiO₂@CNFs

First the *Yucca* leaves were cut into pieces and rinsed with distilled water (DW). 40 g of the shredded leaves was weighed and washed with 2 L of DW and 100 g NaOH at 80 °C for 3 h. After all the green parts were removed, the remaining parts were rinsed with DW until pH reached 7. Finally the white cotton like cellulose can be collected. For the next step 30 mL hydrogen peroxide, 600 mL DW and 10 mL acetic acid was added to cellulose from the

previous step and stirred for 3 h in 80 °C. Then they were washed with DW until pH became neutral, and mixed with 2% HCl, and stirred for next 6 h. By rinsing with DW and drying in oven at 60 °C, CNFs were obtained.

In order to coating CNFs with silica nanoparticles (NPs), a mixture of 200 mg of silica NPs with 80 mg of CNFs and 50 ml of distilled water was sonicated in an ultrasonic bath for 15 minutes and then was stirred for 24 h at room temperature. The SiO₂@CNFs was filtered and dried in oven at 50° C.

1.3. Loading of doxorubicin on the SiO₂@CNFs and releasing experiments

First, a mixture of 200 mg of silica NPs and 80 mg of CNFs in 50 mL DW was sonicated and stirred for 24 h, then 2 mg of doxorubicin was added to the mixture by continues stirring. After 2 h, the drug loading percentage was calculated as 72.6% by measuring the remaining doxorubicin in water after filtration, using UV-Vis spectrophotometer and calibration curve equation: $A = 0.0045 \times C + 0.0078$; where A is the absorbance of solution at $\lambda_{max} = 483$ nm and C is the concentration of doxorubicin. In order to study of the drug release properties, the doxorubicin loaded on SiO₂@CNFs were placed in 20 ml of the prepared buffers and sampled at different times and the release percentage was measured by UV-Vis spectrophotometer. Drug release was investigated in two environments with pH = 4.5 and pH = 7.4, which

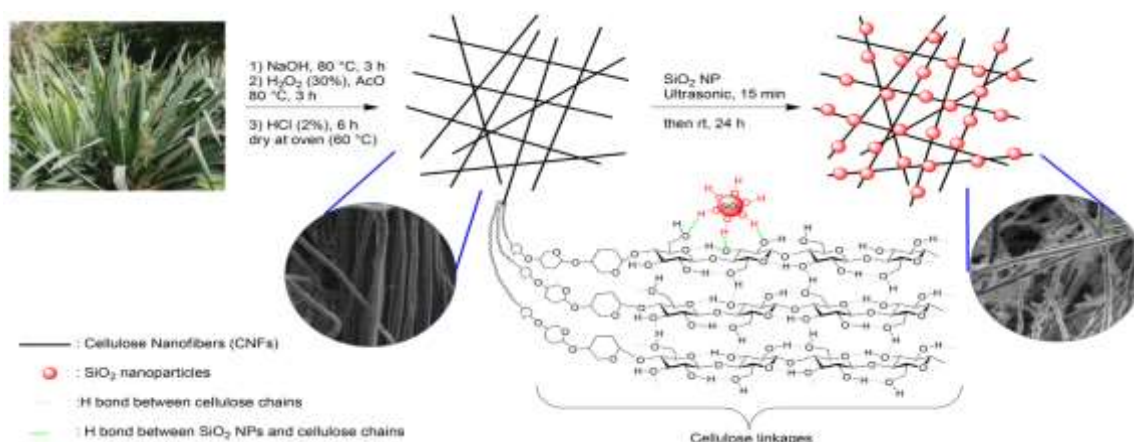


Fig. 1. Schematic representation of the preparation of SiO₂@CNFs were determined to be 73.50% and 17.07%, respectively.

2. Results and discussion

2.1. Preparation of SiO₂@CNFs

Schematic preparation of SiO₂@CNFs is illustrated in Figure 1. Cellulose nanofibers (CNFs) were prepared by extraction from Yucca leaves and bleaching using hydrogen peroxide solution. SiO₂ nanoparticles were immobilized on the surface of CNFs by dispersion of SiO₂ NPs in water using ultrasonic irradiation and then stirring at room temperature in the presence of CNFs for 24 h. Hydrogen bonding between O—H bonds on the surface of SiO₂ NPs and sugars units of cellulose polymeric chains caused the immobilization of SiO₂ NPs on the surface of CNFs.

2.2. FT-IR spectroscopy

FT-IR spectroscopy is used to confirm the chemical structures of the synthesized CNFs and SiO₂@CNFs. Figure 2a shows the spectrum of CNFs, in which a broad absorption peak is observed in 3331 cm⁻¹, relating to the stretching vibration of O—H groups of the CNFs. C—H stretching vibrations of CH and CH₂ groups are appeared at 2851-2942 cm⁻¹. Several absorption peaks are present at 1000–1200 cm⁻¹ which could be attributed to the C—O stretching vibrations of the glucose ring skeletal of the CNFs. The FT-IR spectrum of SiO₂@CNFs is also depicted in Figure 2a. Broad peak at 3006-3712 cm⁻¹ is related to the stretching vibrations of both O—H bonds of alcoholic groups of CNFs and Si—O—H bonds of silica nanoparticles. Broadening that peak in comparison with CNFs is attributed to the formation of intermolecular hydrogen bonding between OH groups of the CNFs and SiO₂. C—H stretching vibrations are appeared at 2889 cm⁻¹, as in the case of CH and CH₂ moieties of CNFs. Peak at 1641 cm⁻¹ is associated with the bending vibration of water molecules, physically adsorbed on the surface of SiO₂ NPs. In addition to the C—O bonds stretching vibration of CNFs, two distinct peaks at 1107 and 802 cm⁻¹ are appeared due to the asymmetric and symmetric modes of Si—O—Si, respectively. The results confirmed the coating of CNFs with SiO₂ nanoparticles.

2.3. X-ray diffraction (XRD)

XRD pattern of SiO₂@CNFs is shown in Figure 2b. Peaks at $2\theta = 15.2, 22.6$ and 34.7° correspond to (1-10), (110) and (200) reflections of the crystalline CNFs, respectively [28, 30]. Broad peak at $2\theta = 22.6^\circ$ could be attributed to the amorphous SiO₂ NPs [31, 32]. Also, low angle XRD pattern of SiO₂@CNFs shows an intense peak at $2\theta = 0.85^\circ$, which is related to the mesoporous structure of SiO₂ nanoparticles (Inset of Figure 2b), indicating well dispersion of SiO₂ NPs on the surface of CNFs.

2.4. TGA analysis

The TGA results of CNFs and SiO₂@CNFs are outlined in Figure 2c. TGA of CNFs indicates the first weight loss below 100 °C (2.78%) that corresponds to the loss of physically adsorbed water molecules. A sharp weight loss at 250–370 °C (75.07%) is attributed to decomposition of organic structure of CNFs. Also about 19.83% slow weight loss is shown between 370 and 580 °C. Totally, about 97.5% weight loss is observed, which indicates that the entire structure of the organic matter is completely burned and destroyed. The TGA of SiO₂@CNFs indicates a similar pattern with TGA of CNFs, in which mass loss at 90–110 °C (3.66%) corresponds to the loss of physically adsorbed water. Also, the thermal decomposition of organic section of SiO₂@CNFs at 260–410 °C is the main and important weight loss (56.65%), which is about 37% less than pure CNFs. Also there is no considerable weight loss even at high temperature (900 °C), confirming that the SiO₂ NPs is deposited on the cellulose fibers and remains unchanged.

2.5. SEM and TEM analysis

Surface morphology and textural properties of CNFs and SiO₂@CNFs are investigated by SEM and TEM images. SEM analysis of CNFs shows fibrillar structure (Figure 2e). As shown in Figure 2f, in the case of SiO₂@CNFs, fibrillar structure of CNFs is also shown, in which CNFs are coated with SiO₂ nanoparticles. Formation of compact SiO₂ spherical nanoparticles with average diameter of 20 nm on the surface of CNFs is confirmed. In order to investigate elemental analysis of the prepared CNFs and SiO₂@CNFs, energy dispersive X-ray (EDX) analysis is performed (Figure 2d). EDX data of CNFs shows the presence of C and O atoms in the structure. While, in

addition to C and O, Si is also shown in the EDX analysis of SiO₂@CNFs. The shape and size of the CNFs and SiO₂ NPs on the fibers are studied using TEM analysis. TEM image of SiO₂@CNFs is shown in Figure 2g, in which an uneven distribution of SiO₂ spherical NPs on the surface of CNFs is observed.

2.6. Doxorubicin release studies

Doxorubicin, an anticancer drug, is selected in order to study the practical applications of the prepared

SiO₂@CNFs in drug delivery systems. Loading Level (LL) of drug into carriers is one of the most important factors in drug delivery systems, as a high LL makes the carriers to be more desirable. The LLs of CNFs and SiO₂@CNFs toward doxorubicin are found to be 79.82% and 72.67%, respectively. It was found that the LL of the SiO₂@CNFs is lower than CNFs. It could be attributed to the coating of CNFs with SiO₂

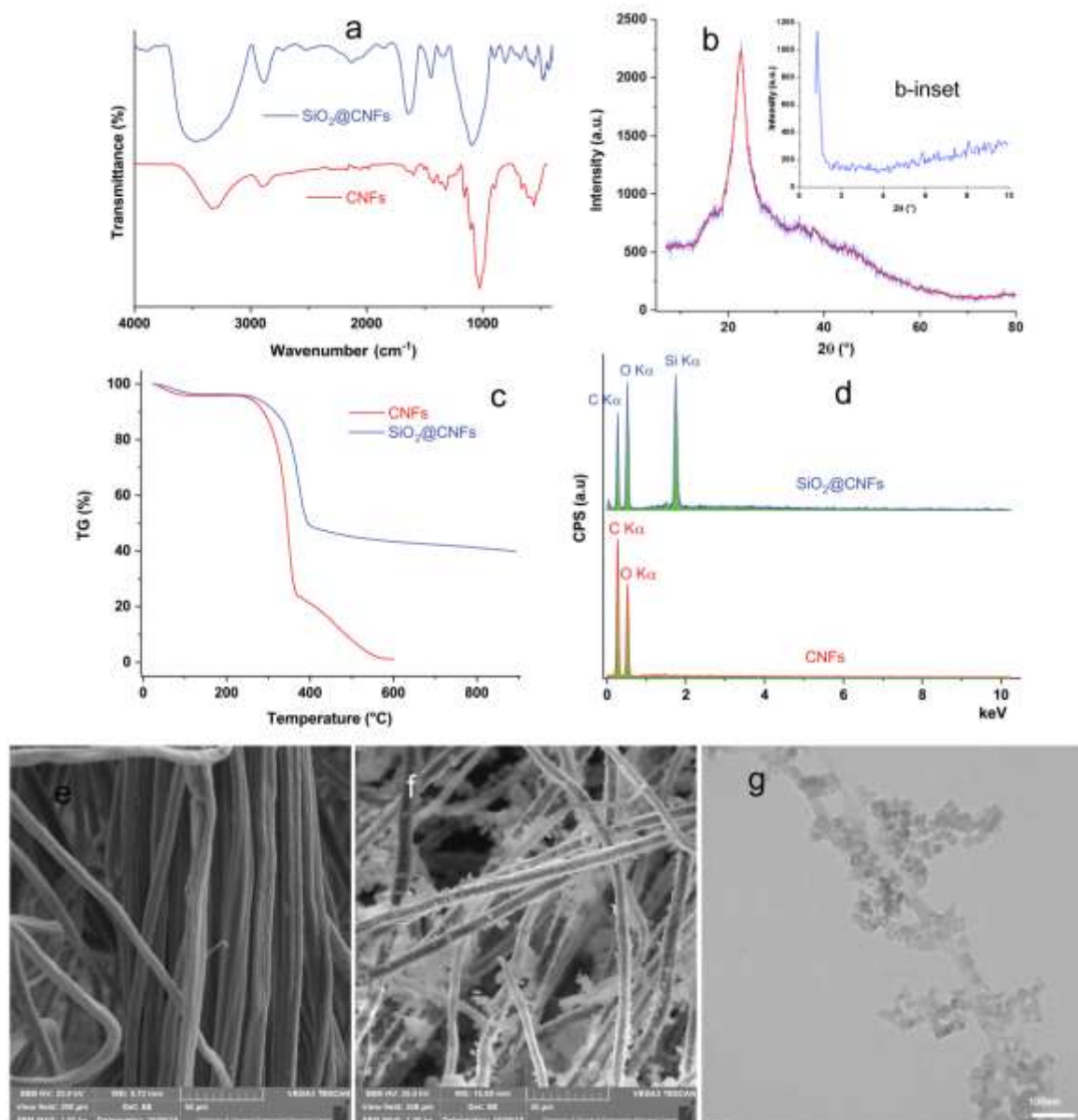


Fig. 2. (a) FT-IR spectra of CNFs and SiO₂@CNFs, (b, and b-inset) wide angle and low angle XRD pattern of SiO₂@CNFs, (c) TGA analysis of CNFs and SiO₂@CNFs, (d) EDX analysis of CNFs and SiO₂@CNFs, (e) SEM image of CNFs, (f) SEM image of SiO₂@CNFs and (g) TEM image of SiO₂@CNFs (Scale Bar = 100 nm).

nanoparticles, which occupy the active sites of the CNFs. Then, *in vitro* doxorubicin release of CNFs and SiO₂@CNFs was investigated. The effect of the pH value on the release of doxorubicin from the NFC was studied.

The doxorubicin release profiles at pH values of 4.5 and 7.4 versus time are illustrated in Figure 3. At both pH values, CNFs shows rapid cumulative release (CR%) of the doxorubicin (about 94% over 5 h, and 88% over 7.5

h, at pH values of 4.5 and 7.4, respectively), approving that the CNFs is not an ideal candidate for drug release. To overcome this problem, CNFs were coated with SiO₂ nanoparticles to control release of doxorubicin. As shown in Figure 3, release of doxorubicin from SiO₂@CNFs occurs slowly at both pH values of 4.5 and 7.4. This could be attributed to the encapsulating properties of SiO₂ nanoparticles on the surface of CNFs, inhibiting the permeability of doxorubicin in the solution.

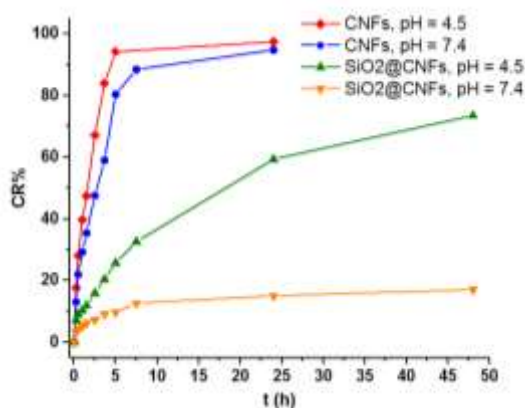


Fig. 3. Profiles of doxorubicin release from CNFs and SiO₂@CNFs at pH values of 4.5 and 7.4 versus time.

However, due to the pH-sensitivity of the doxorubicin release from SiO₂@CNFs, their high content of drug release at pH = 4.5 was expected, which could be associated with the basic properties of doxorubicin with pK_b value of 5.78 (pK_a of conjugated acid is 8.22), leading to the formation of ammonium salt of doxorubicin at lower pH values and therefore higher solubility in aqueous medium. The structure of doxorubicin and its protonated form in acidic medium are illustrated in Figure 4a. Also, at lower pH value protonated water molecules penetrated into the pores of the nanocomposite, leading to the repulsion with ammonium salt of doxorubicin, and therefore higher content of drug release. The interaction of doxorubicin molecule with the surface of SiO₂@CNFs by hydrogen bonding at pH = 7.4 (top) and pH = 4.5 (bottom) are depicted in Figure 4b. Over 48 h, low release content (17.07%) is observed for the SiO₂@CNFs at pH = 7.4, while 73.50% cumulative release percentage was observed at pH = 4.5.

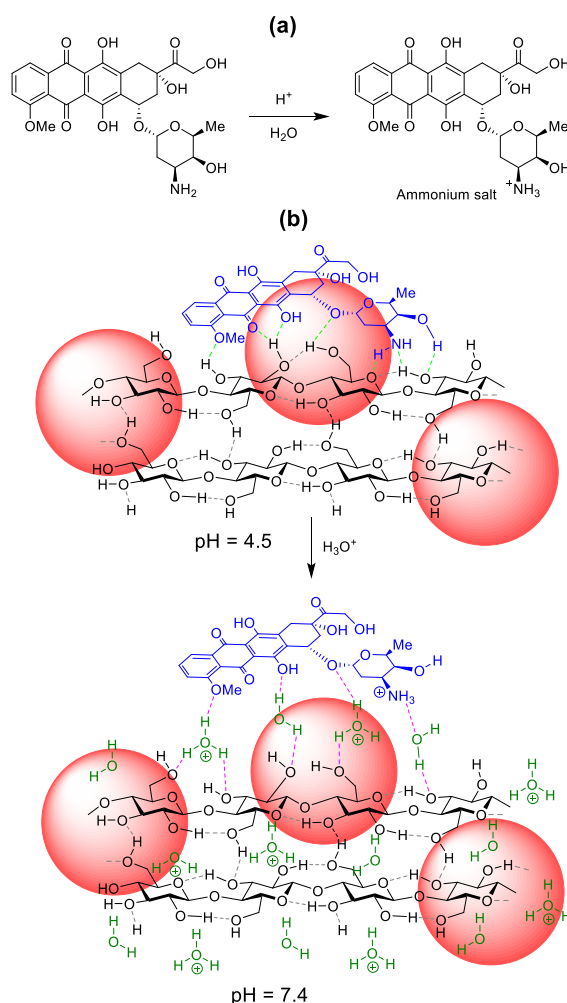


Fig. 4. Structure of doxorubicin and its protonated form in acidic medium.

In order to understand drug release profile, the experimental data of the doxorubicin release from CNFs and SiO₂@CNFs at both pH values were modeled according to the some commonly used kinetic models,[33, 34] including:

(i) *Zero order* model, expressed as equation (1)

$$Q_t = Q_0 + k_0 t \quad (1)$$

Where, Q_0 , Q_t , k_0 and t are the initial amount of drug in the solution (mostly $Q_0 = 0$), cumulative amount of drug released at time t , zero-order rate constant and time, respectively. To investigate the zero order kinetic, the experimental data are plotted as cumulative percentage (CR%) of drug release versus time, in which k_0 is calculated from the slope of the obtained line.

(ii) *First order* model, represented as equation (2)

$$\log C_t = \log C_0 + k_1 t / 2.303 \quad (2)$$

Where, C_0 , C_t , k_1 and t are the initial amount of drug, cumulative amount of drug remaining, first order rate constant and time, respectively. Plotting the log cumulative percentage of drug remaining (100-CR%) versus time is used to study the first order kinetic, in which $k_1/2.303$ is slope of the yielded line.

(iii) *Higuchi model*, expressed as equation (3)

$$Q_t = K_H t^{1/2} \quad (3)$$

Where, Q_t and t are as assigned above, and k_H is the Higuchi dissolution constant. By plotting cumulative percentage (CR%) drug release versus square root of time, the Higuchi dissolution constant (k_H) was obtained from slope of the obtained line.

(iv) *Korsmeyer–Peppas model*, stated as equation (4)

$$M_t/M_\infty = K_{KP} t^n \quad (3)$$

Where M_t/M_∞ is the fraction of drug released at time t , and k_{KP} and n are the release rate constant and release exponent, respectively. Release exponent (n) indicates the release mechanism of drug. The values of $n \leq 0.45$ and $0.45 < n < 0.89$ corresponds to a Fickian type diffusion (diffusion kinetic) and nonFickian (diffusion kinetic and polymer relaxation kinetic), respectively.[35, 36] To study Korsmeyer–Peppas model, log cumulative percentage (CR%) of drug release are plotted versus log time. k_{KP} and n were obtained from $10^{\text{intercept}}$ and slope of the obtained line, respectively.

(v) *Hixson–Crowell model*, expressed as equation (5)

$$W_0^{1/3} - W_t^{1/3} = k_{HC} t \quad (5)$$

Where, W_0 and W_t are the initial amount of drug and the remaining amount of drug at time t , respectively, and k_{HC} is a constant, that combined the relation between surface and volume. The model was studied by plotting cube root of drug amount remaining in system $[(1-\text{CR})^{1/3}]$ versus time, in which k_{HC} is the slope of the obtained line.

(vi) *Weibull model*, described as equation (6)

$$M_t = M_0(1 - e^{(-b \times t^a)}) \quad (6)$$

Where, M_0 and M_t are the total amount of drug being released and the amount of drug released at time t . Factors of a and b indicate a scale parameter, describing the time dependence, and the shape of dissolution curve progression. This model was studied by linear plotting $\text{Ln}[-\text{Ln}(1-\text{CR})]$ versus $\text{Ln}(t)$, in which CR is cumulative

amount of release, and a is slope of the obtained line, and b is calculated by $b = e^{(\text{intercept})}$.

(vii) *Gompertz model*, described as equation (7)

$$Q_t/Q_0 = e^{(\alpha \cdot e^{(\beta \cdot \log t)})} \quad (7)$$

Where, Q_0 , Q_t and t are as assigned above, α is scale parameter, which indicates the undissolved portion at time $t = 1$, and β is shape parameter, which indicates the dissolution rate per unit of time. Linear plot of $\text{Ln}[\text{Ln}(\text{CR}\%)]$ versus $\text{Ln}(t)$ is used to study this type of kinetic model, in which CR% is cumulative percentage of release, and α and β were calculated by $e^{(\text{intercept})}$ and $2.303 \times \text{slope}$, respectively.

Linear fitting the experimental data with corresponding kinetic models are shown in Figure 5. Also calculated release constant and parameters are summarized in Table 1.

Fitting the experimental data with different models revealed that doxorubicin release from CNFs at pH value of 4.5, is fitted with Higuchi and Korsmeyer–Peppas as well as Hixson–Corwell models, with the regression coefficients (r^2) 0.9982, 0.9966 and 0.9990, respectively. Release at pH 7.4 is also well fitted with Higuchi, Korsmeyer–Peppas and Hixson–Corwell models with $r^2 = 0.9946$, 0.9914 and 0.9983, respectively. Higuchi model was applied for drug release systems, in which drug delivery occurred via both dissolution and diffusion process.[37] This phenomenon was frequently shown when the initial drug concentration in the drug release system is much higher than the solubility of the drug, and/or the matrix is slightly swelled or dissolved. Korsmeyer–Peppas model indicates the primary mechanism of drug delivery is controlled by diffusion process and also which type of diffusion is dominant [38]. By fitting the experimental data using Korsmeyer–Peppas equation, n values for the release of doxorubicin from CNFs are obtained to be 0.5566 at pH = 4.5 and 0.5586 at pH = 7.4, revealing the nonFickian diffusion kinetic. While, the Hixson–Crowell model applies when the dissolution of drug occurs in planes that are parallel to the surface of the active agent, which caused to change in surface area and diameter of the drug delivery system.[34]

Doxorubicin delivery from SiO₂@CNFs is slower than CNFs at both pH values of 4.5 and 7.4, as k values for the delivery from SiO₂@CNFs in all studied models (Table 1) are lower than values for drug release form CNFs system at both pH values. However release at pH = 4.5 is higher and faster than pH = 7.4. As shown in Figure 5 and according to the data of Table 1, release from SiO₂@CNFs at pH = 4.5 follows Higuchi and Hixson–Crowell models with regression coefficient (r^2) of 0.9954 and 0.9978, respectively. The n value of 0.4755 obtained

from Korsmeyer-Peppas model indicates nonFickian diffusion kinetic for release of doxorubicin from SiO₂@CNFs at pH = 4.5. Experimental data of release from SiO₂@CNFs at pH = 7.4 is well fitted with Hixson–Crowell model with $r^2 = 0.9996$, indicating the change of surface area of drug release system by dissolution and diffusion of drug into the solution. The n value for the Korsmeyer-Peppas model is calculated to be 0.3359, indicating Fickian type diffusion of doxorubicin into the solution from SiO₂@CNFs drug delivery system.

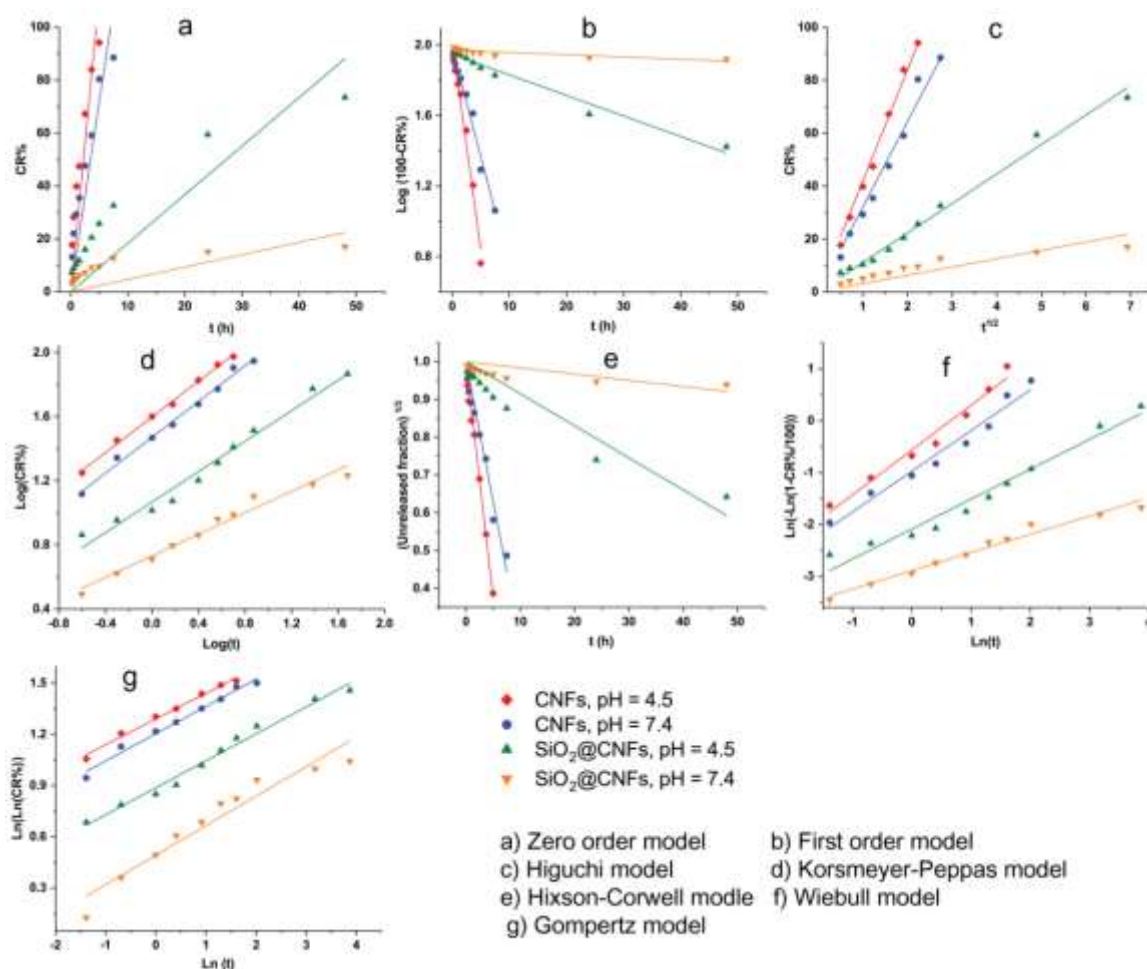


Fig. 5. Linear fitting the experimental data with various kinetic models.

Table 1. Calculated release constant and parameters.

Model	Parameters	CNFs		SiO ₂ @CNFs	
		pH = 4.5	pH = 7.4	pH = 4.5	pH = 7.4
Zero order	k_0	22.3098	14.3307	1.8351	0.4671
$Q_t = Q_0 + k_0 t$	r^2	0.9456	0.9410	0.8579	0.6487
First order	k_1	0.5410	0.2832	0.02685	0.002948
$\log C_t = \log C_0 + k_1 t / 2.303$	r^2	0.9780	0.9778	0.9744	0.7436
Higuchi	k_H	41.9353	32.1737	11.1432	3.1409
$Q_t = K_H t^{1/2}$	r^2	0.9982	0.9946	0.9954	0.9229
Korsmeyer-Peppas	k_{KP}	39.5867	29.5631	11.6600	5.3872

$M_t/M_\infty = k_{KP}t^n$	n	0.5566	0.5586	0.4755	0.3359
	r^2	0.9966	0.9914	0.9781	0.9730
Hixson-Corwell	k_{HC}	-0.1250	-0.0740	-0.0085	-0.00165
$W_0^{1/3} - W_t^{1/3} = k_{HC}t$	r^2	0.9990	0.9983	0.9978	0.9996
Weibull	a	0.8632	0.7835	0.5763	0.3513
$M_t = M_0(1 - e^{(-b \times t^a)})$	b	0.5689	0.3773	0.1240	0.05550
	r^2	0.9722	0.9692	0.9675	0.9753
Gompertz	α	3.6344	3.3341	2.4274	1.6363
$Q_t/Q_0 = e^{(\alpha \cdot e^{(\beta \cdot \log t)})}$	β	0.3472	0.3677	0.3642	0.3982
	r^2	0.9896	0.9843	0.9845	0.9329

3. Conclusion

In conclusion, cellulose nanofibers were extracted from *Yucca* leaves and then coated by SiO₂ nanoparticles. Characterization of the prepared SiO₂@CNFs revealed the immobilization of SiO₂ nanoparticles on the cellulose nanofibers. Both CNFs and SiO₂@CNFs were investigated to controlled delivery of doxorubicin. CNFs itself release the doxorubicin rapidly within 5-7 h at both studied pH values, while immobilization of SiO₂ NPs on the surface of CNFs approved its drug delivery properties. Delivery of doxorubicin from SiO₂@CNFs demonstrated excellent pH-sensitivity and can be considered as a good carrier for doxorubicin controlled release. The cumulative release percentage of doxorubicin was measured to be 73.5% at pH = 4.5, and the content of released doxorubicin was considerably decreased at pH = 7.4 (17.07% cumulative release percentage). According to the regression coefficients (r^2), the kinetic data was well-fitted with the Higuchi, Korsmeyer-Peppas and Hixson-Corwell models in the case of release from CNFs at both pH values, while release from SiO₂@CNFs follows Higuchi and Hixson-Crowell models at pH = 4.5 and Hixson-Crowell model at pH = 7.4. In addition, the n values obtained by fitting experimental data with Korsmeyer-Peppas model revealed that the transport mechanism of the doxorubicin from the CNFs at both pH values and SiO₂@CNFs at pH = 4.5 was nonFickian diffusion type kinetic, while release from SiO₂@CNFs at pH = 7.4 occurred by Fickian type diffusion.

Acknowledgments

We are grateful to the Payame Noor University for financial support.

References

- [1] A. Deshpande, C. Rhodes, N. Shah, and A. Mallick, *Drug Dev. Ind. Pharm.* **22** (1996) 531.
- [2] E. Einafshar, A. Haghighi Asl, M. Ramezani, A. Hashemnia, and A. Malekzadeh, *Adv. Drug Deliv. Rev.* **60** (2008) 548.
- [3] G.R. Mahdavinia, S. Ettehadi, M. Amini, and M. Sabzi, *RSC Advances* **5** (2015) 44516.
- [4] F. Khanmohammadi, B.M. Razavi Zadeh, and S.N. Azizi, *Applied Chemistry* (2022).
- [5] S. Salmanpour, M.A. Khalilzadeh, D. Zareyee, and H. Karimi-Maleh, *Applied Chemistry* **15** (2020) 9.
- [6] R. Kolakovic, L. Peltonen, A. Laukkanen, J. Hirvonen, and T. Laaksonen, *Eur. J. Pharm. Biopharm.* **82** (2012) 308.
- [7] G. Rezanejade Bardajee, S. Asgari, and S. A. Mirshokraei, *Iran. J. Chem. Chem. Eng.* **40** (2021) 1386.
- [8] S. J. Tabatabaei Rezaei, A. Mashhadi Malekzadeh, L. Sarbaz, H. Niknejad, and A. Ramazani, *J. Appl. Chem.* **15** (2020) 55.
- [9] Z. Ali Mardan, and M. Darabi, *J. Appl. Chem.* **10** (2015) 29.
- [10] H. Hosseinzadeh, *J. Appl. Chem.* **6** (2011) 21.
- [11] G. R. Mahdavinia, A. Afzali, H. Etemadi, H. and Hoseinzadeh, *Nanomed. Res. J.* **2** (2017) 111.
- [12] M. Zirak, A. Abdollahiyan, B. Eftekhari-Sis, and M. Saraei, *Cellulose* **25** (2018) 503.

- [13] M. Kianfar, and A. Mohammadi, *Applied Chemistry* **15** (2020) 163.
- [14] P. Stenstad, M. Andresen, B. S. Tanem, and P. Stenius, *Cellulose* **15** (2008) 35.
- [15] T. Zimmermann, N. Bordeanu, and E. Strub, *Carbohydr. Polym.* **79** (2010) 1086.
- [16] A. Chakraborty, M. Sain, and M. Kortschot, *Holzforchung* **59** (2005) 102.
- [17] H. Valo, S. Arola, P. Laaksonen, M. Torkkeli, L. Peltonen, M. B. Linder, R. Serimaa, S. Kuga, J. Hirvonen, and T. Laaksonen, *Eur. J. Pharm. Sci.* **50** (2013) 69.
- [18] J. Hu, H. -Y. Li, G. R. Williams, H. -H. Yang, L. Tao, and L. -M. Zhu, *J. Pharm. Sci.* **105** (2016) 1104.
- [19] A. Allafchian, H. Hosseini, and S. M. Ghoreishi, *Int. J. Bio. Macromol.* **163** (2020) 1780.
- [20] K. Löbmann, and A. J. Svagan, *Int. J. Pharm.* **533** (2017) 285.
- [21] M. Arruebo, M. Galán, N. Navascués, C. Téllez, C. Marquina, M. R. Ibarra, and J. Santamaría, *Chem. Mater.* **18** (2006) 1911.
- [22] M. Kundu, S. Chatterjee, N. Ghosh, P. Manna, J. Das, and P. C. Sil, *Mater. Sci. Eng. C* **116** (2020) 111239.
- [23] M. Lin, H. Wang, S. Meng, W. Zhong, Z. Li, R. Cai, Z. Chen, X. Zhou, and Q. Du, *J. Pharm. Sci.* **96** (2007) 1518.
- [24] R. Thenmozhi, M. S. Moorthy, J. Sivaguru, P. Manivasagan, S. Bharathiraja, Y. -O. Oh, and J. Oh, *J. Nanosci. Nanotechnol.* **19** (2019) 1951.
- [25] C. A. McCarthy, R. J. Ahern, R. Dontireddy, K. B. Ryan, and A. M. Crean, *Expert Opin. Drug Deliv.* **13** (2016) 93.
- [26] Y. Chen, H. Chen, and J. Shi, *Expert Opin. Drug Deliv.* **11** (2014) 917.
- [27] T. T. H. Thi, T. N. Q. Nguyen, D. T. Hoang, and D. H. Nguyen, *Mater. Sci. Eng. C* **99** (2019) 631.
- [28] Y. Liu, Y. Peng, T. Zhang, F. Qiu, and D. Yuan, *Cellulose* **25** (2018) 3067.
- [29] J. I. Morán, V. A. Alvarez, V. P. Cyras, and A. Vázquez, *Cellulose* **15** (2008) 149.
- [30] S. Zhou, V. Apostolopoulou-Kalkavoura, M. V. T. da Costa, L. Bergström, M. Strømme, and C. Xu, *Nano-Micro Lett.* **12** (2020) 1.
- [31] H. El-Didamony, K. A. Khalil, I. Ahmed, and M. Heikal, *Constr. Build. Mater.* **35** (2012) 77.
- [32] J. Sun, Z. Xu, W. Li, and X. Shen, *Nanomaterials* **7** (2017) 102.
- [33] S. Dash, P. N. Murthy, L. Nath, and P. Chowdhury, *Acta Pol. Pharm.* **67** (2010) 217.
- [34] M. L. Bruschi, *Strategies to modify the drug release from pharmaceutical systems*, Woodhead Publishing (2015).
- [35] P. L. Ritger, and N. A. Peppas, *J. Control. Releas.* **5** (1987) 23.
- [36] P. L. Ritger, and N. A. J. Control. Releas. **5** (1987) 37.
- [37] H. Omidian, and K. Park, *Introduction to hydrogels, Biomedical applications of hydrogels handbook*, Springer (2010) 1.
- [38] N. Peppas, *Pharm. Acta Helv.* **60** (1985) 110.